

The intercalation of cetyltrimethylammonium cations into muscovite by a two-step process: I. The ion exchange of the interlayer cations in muscovite with Li^+

Xiaofeng Yu^a, Liyan Zhao^a, Xiuxiang Gao^b, Xiaoping Zhang^c, Nianzu Wu^{a,*}

^aState Key Laboratory for Structural Chemistry of Unstable and Stable Species, Institute of Physical Chemistry, Peking University, Beijing 100871, China

^bLaboratory Center, Research Institute of Petroleum Exploration and Development, PetroChina, P.O. Box 910, Beijing 100083, China

^cElectron Microscopy Laboratory, Peking University, Beijing 100871, China

Received 7 December 2005; received in revised form 1 February 2006; accepted 5 February 2006

Available online 20 March 2006

Abstract

A new method to prepare alkylammonium ions-intercalated muscovite is reported. It has been obtained in a two-step process: the first step is the inorganic ion exchange, which allows the ion exchange of interlayer cations in muscovite with Li^+ in a melting condition of LiNO_3 . It was found that in the LiNO_3 treatment process most of the interlayer cations were replaced by Li^+ , and a large amount of water entered the interlayer space of muscovite. Therefore the spacing of muscovite (001) plane $d_{(001)}$ was enlarged from 19.92 to 24.16 Å, which could allow for the intercalation of organic cations. SEM shows that the LiNO_3 treatments have little effect on the size of muscovite platelets. TEM and FTIR confirm that not only the chemical composition but also the structure of the aluminosilicate layer has not been changed by the LiNO_3 treatments.

© 2006 Elsevier Inc. All rights reserved.

Keywords: Layered silicate; Muscovite; Ion exchange; Intercalation

1. Introduction

Layered compounds have attracted increased research attention due to their applications in many fields. The intercalation of organic species into the interlayer space of layered silicate has been studied extensively because the resulting intercalates have interesting properties and have many applications in a range of key areas, such as adsorbents for organic pollutants [1], catalysts [2], rheological control agents [3], reinforcement phase in polymer matrices [4], drug carrier in pharmaceutical field [5], photofunctional materials [6] and so on.

The ion-exchange intercalation of organic cations into silicate is a result of interplay of several factors: the density of layer charge, the degree of exchange, the length of the alkyl chain, and the host–guest and guest–guest interactions [7,8]. In the 2:1 layered silicate, smectite and

vermiculite have been most investigated as host materials in the intercalation because of their swelling behavior and ion exchange properties [9]. However, another important silicate group, mica (especially muscovite), has attracted much less attention. Muscovite is a clay mineral of special interest because of its well-defined crystal structure, molecularly smooth surface, and outstanding corona resistance [10]. Muscovite belongs to monoclinic structure with the space group ($C2/c$), with the cell parameter $a = 5.18 \text{ \AA}$, $b = 8.99 \text{ \AA}$, $c = 20.07 \text{ \AA}$, $\beta = 95.75^\circ$ [11]. There are two aluminosilicate layers along the [001] direction in one cell unit. Although muscovite belongs to 2:1 phyllosilicate, it has a few distinct differences compared with smectite and vermiculite. First of all, it has very high layer charge density of $2e$ in half unit cell [$\text{O}_{20}(\text{OH})_4$]; secondly, it has homogeneous charge distribution; in addition, its layer charge comes from the outside tetrahedral sheet of the aluminosilicate layer and hence produces much strong electrostatic force to hold aluminosilicate layers and the interlayer cations together. Therefore, muscovite does not

*Corresponding author. Fax: +86 10 62754943.

E-mail address: wunz@pku.edu.cn (N. Wu).

swell in water; the ion exchange and intercalation, which smectite and vermiculite groups usually have, is not so easy for muscovite. Considering the unique characteristics of muscovite, it will be very interesting if the organic compound intercalation based on muscovite could be obtained.

For synthetic mica, the interlayer cations could be exchanged by other inorganic ions [12]. Komarneni studied thoroughly the cation exchange of synthetic mica with alkali and alkaline earth metal cations [13] and transition metal ions [14]. However, the ion exchange of muscovite was not easily performed. Bracke et al. [15] found a method to carry out the cations exchange on phlogopite, biotite, and muscovite using cryptand [222] as a complexing agent, dioxane as solvent, and Li as the exchange cations. The results indicate greater than 90% exchange of the analyzed cations K^+ , Rb^+ , and Sr^+ in phlogopite and biotite after 2 days. Similar results for the exchange in muscovite are observed but it is apparently slower. Suter prepared partially delaminated muscovite with high specific surface area by treating muscovite powder with hot saturated lithium nitrate solution [16] and got alkane monolayer self-assembled on this delaminated muscovite [17]. Enlightened by their work, we developed a new method to prepare muscovite with very high specific surface area by melting $LiNO_3$ [18]. Furthermore, it has been found in the present paper that the basal spacing of muscovite can be fully enlarged after $LiNO_3$ treatments, which provides great possibility for the intercalation of organic cations into the interlayer of muscovite by ion exchange. In the present paper, we prepared the $LiNO_3$ -treated muscovite as the host for the alkylammonium intercalation. It was found that most of the interlayer cations were replaced by hydrated Li^+ ; the chemical composition and the structure of the aluminosilicate layer have not been changed by the $LiNO_3$ treatments.

2. Experimental

2.1. The $LiNO_3$ treatment of muscovite

The chemical formula of the original muscovite powder ($2M_1$, from Nanling region, China) is $(K_{1.7}Na_{0.3})(Al_{3.54}Fe_{0.26}Mg_{0.20})(Si_{6.20}Al_{1.80})O_{20}(OH)_4$. 10 g muscovite powder and 170 g $LiNO_3$ powder were mechanically mixed. After complete mixing, the mixture was heated in furnace at $300^\circ C$ for 12 h. The resulting product was washed with deionized water and filtered, and then dried at $110^\circ C$. The $LiNO_3$ treatment was repeated for seven times. The product is named Li-muscovite.

2.2. Characterization

The Powder X-ray Diffraction (XRD) patterns were obtained on a Rigaku Rotaflex X-ray powder diffractometer equipped with a graphite-crystal monochromator for $CuK\alpha$ (Ni filter) radiation. The accelerating voltage was

40 kV and the anode current was 100 mA. The wide-angle diffraction patterns in the 2θ range from 2.5° to 130° were collected with a step size of 0.01° and data acquisition time of 4 s. The small-angle diffraction patterns from 1° to 10° were collected using a step-scanning speed of $0.02^\circ/s$.

Middle-infrared transmission spectra ($650\text{--}4000\text{ cm}^{-1}$) were collected using a Nicolet Magna-IR 750 Fourier transform infrared spectrometer equipped with a Nicolet NicPlan IR Microscope operated with a spectral resolution of 4 cm^{-1} . Far-infrared spectra ($50\text{--}650\text{ cm}^{-1}$) were collected using a Nicolet Magna-IR 750 Fourier transform infrared spectrometer with a spectral resolution of 8 cm^{-1} .

High-resolution transmission electron microscopy (HRTEM) studies were performed using a Philips Tecnai F30 high-resolution field-emission transmission electron microscope operating at 300 kV, and equipped with energy-dispersive X-ray spectroscopy (EDX). TEM samples were prepared by dispersing the powder in alcohol by ultrasonic treatment, dropping onto a porous carbon film supported on a copper grid, and then dried in air. The SEM studies were performed on KYKY1000B scanning electron microscope.

Inductively coupled plasma (ICP) emission spectroscopic data were acquired by ICAP-9000 SP instrument of JARRELL-Ash Company.

3. Results and discussions

After the $LiNO_3$ treatment at $300^\circ C$ for 12 h, the structure of muscovite was greatly changed. Fig. 1 shows that after the first $LiNO_3$ treatment some new diffraction peaks (marked by asterisk *) appeared. With the increase of $LiNO_3$ treatment times, the relative intensities of the new peaks become more and more strong, while the peaks of original muscovite become weak. After seven $LiNO_3$ treatments, almost all the original peaks disappeared, and

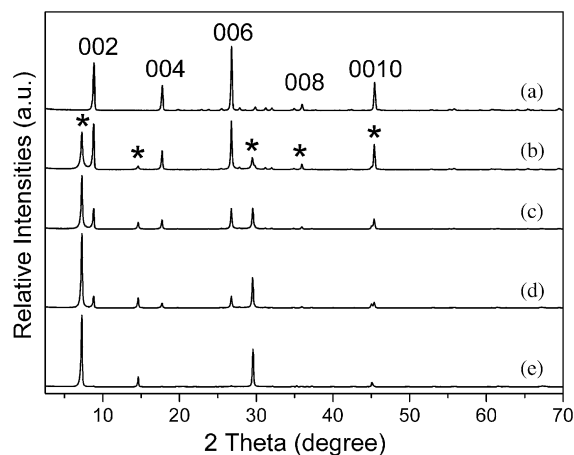


Fig. 1. Powder XRD diffraction patterns of (a) original muscovite, (b) muscovite after the first $LiNO_3$ treatment, (c) muscovite after the second $LiNO_3$ treatment, (d) muscovite after the third $LiNO_3$ treatment, (e) muscovite after the seventh $LiNO_3$ treatment.

the diffraction patterns were composed of a new series of diffraction lines.

This phenomenon does not mean that a brand-new compound has been produced. Because of the strong preferred-orientation of the muscovite crystallites during the powder XRD data collection, the (00 l) diffraction lines are the prominent lines, as shown in pattern a, Fig. 1. For the Li-muscovite's first few new lines with d values of 12.09, 6.05, 4.03, 3.02, 2.41 Å, their d values are in line with the relationship $d_{002} = 2d_{004} = 3d_{006} = 4d_{008} = 5d_{0010}$. Therefore, the spacing of (001) plane $d_{(001)}$ was enlarged from 19.92 to 24.16 Å after the LiNO₃ treatments (shown in Fig. 2). However, the intensity of 006 line in Li-muscovite is very weak. The intensity of some diffraction line is directly proportional to the square of structure factors. Therefore, three factors, the cell parameter, the atom species, and the atom fractional coordinate, could affect the intensity. Because most of the interlayer cations were replaced by Li⁺ (shown in Table 1), and the spacing of (001) plane $d_{(001)}$ was enlarged, all the three factors were changed. So the intensity of (00 l) diffraction lines changed dramatically, which should be the reason of the very weak intensity of 006 line.

The ICP results show that after the LiNO₃ treatment, some K⁺ situated in the interlayer of muscovite are lost and there are many Li⁺ appearing in the product as shown in Tables 1 and 2. Even after seven LiNO₃ treatments, the contents of the Si, Al, Fe and Mg, which compose the aluminosilicate layer, are almost unchanged, and the amount of Li⁺ is equal to the amount of lost K⁺ and Na⁺.

Fig. 3 shows the selected area electron diffraction (SAED) patterns along the [001] direction and EDX spectra of the original muscovite and the muscovite after the seven LiNO₃ treatments. From the SAED patterns it could be obtained that before and after LiNO₃ treatments muscovite has almost the same ($hk0$) patterns. The calculated crystal parameters are $a = 5.18$ Å, $b = 9.00$ Å for both the original muscovite and LiNO₃-treated

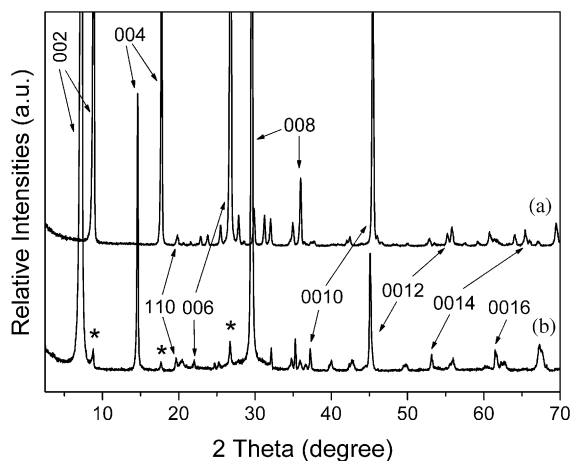


Fig. 2. The diffraction patterns of (a) original muscovite and (b) muscovite after the seventh LiNO₃ treatment; the peaks marked by asterisk are the remainder of the original muscovite.

Table 1

The chemical composition (wt%) of original muscovite and LiNO₃-treated muscovite

Element oxide	Original muscovite	Muscovite after first LiNO ₃ treatment	Muscovite after seven LiNO ₃ treatment
SiO ₂	46.6	47.3	47.9
Al ₂ O ₃	34.1	34.6	35.0
Fe ₂ O ₃	2.6	2.5	2.7
MgO	1.0	1.1	1.0
K ₂ O	10.0	6.8	2.4
Na ₂ O	1.2	0.8	0.3
Li ₂ O	0	1.2	2.9
Loss in calcination	4.4	5.7	7.7

muscovite, indicating that the LiNO₃ treatment has no influence on the skeleton structure of the aluminosilicate layer. The EDX spectra show the main elements (Si, Al, O, K) of original muscovite and LiNO₃-treated muscovite. It is very clear that after seven LiNO₃ treatments the chemical composition of Si, Al, and O remains the same as that in the original muscovite, however almost all the K⁺ disappear. Thus the SAED patterns and the EDX spectra reveal that both the chemical composition and the structure of the aluminosilicate layer has not been changed by the LiNO₃ treatments, and almost all the K⁺ in the interlayer have been lost. The diffraction line of d_{110} , which has no relation to the change of parameter c , remains constant as shown in Fig. 2, also indicating the crystal parameters a and b have not been affected.

Fig. 4 shows the far- and middle-infrared spectra of original muscovite and muscovite after the seventh LiNO₃ treatment. The assignment of the bands is shown in Table 3 [19,20]. It could be obtained that most absorption bands in the spectrum of the LiNO₃-treated muscovite, especially the bands of Si–O stretching and bending vibration, are similar to that of original muscovite, indicating that the structure of the aluminosilicate layer remains the same after the LiNO₃ treatments. The first change is that the absorption band of K⁺ at 110 cm⁻¹ in the original muscovite spectrum becomes very weak, indicating that most of the K⁺ are lost after the LiNO₃ treatments. According to the relationship between the frequency and $\sqrt{Z/m}$, where Z is the charge and m the mass of the cation, the band of Li⁺ should be in the range of 200–300 cm⁻¹ [20]. So the absorption band of Li⁺ may overlap the strong band between 200 and 600 cm⁻¹ and could not be observed. The second change is that new bands at 3430, 3270, and 1642 cm⁻¹ emerge, indicating that large amounts of H₂O enter the interlayer of aluminosilicate layers [19]. In addition, the bands at 925, 410, 350, and 262 cm⁻¹ become less prominent after the LiNO₃ treatment, and this may be due to the hydration of the cations in the interlayer and the interaction between water and aluminosilicate layer. It could be obtained from infrared spectra that the

Table 2
Chemical formula of original muscovite and LiNO₃-treated muscovite

Sample	Formula
Original muscovite	$(K_{1.7}Na_{0.3})(Al_{3.54}Fe_{0.26}Mg_{0.20})(Si_{6.20}Al_{1.80})O_{20}(OH)_4$
Muscovite after first LiNO ₃ treatment	$(K_{1.14}Na_{0.20}Li_{0.66})(Al_{3.54}Fe_{0.25}Mg_{0.21})(Si_{6.20}Al_{1.80})O_{20}(OH)_4(H_2O)_{0.56}$
Muscovite after seven LiNO ₃ treatment	$(K_{0.40}Na_{0.08}Li_{1.52})(Al_{3.54}Fe_{0.26}Mg_{0.20})(Si_{6.20}Al_{1.80})O_{20}(OH)_4(H_2O)_{1.32}$

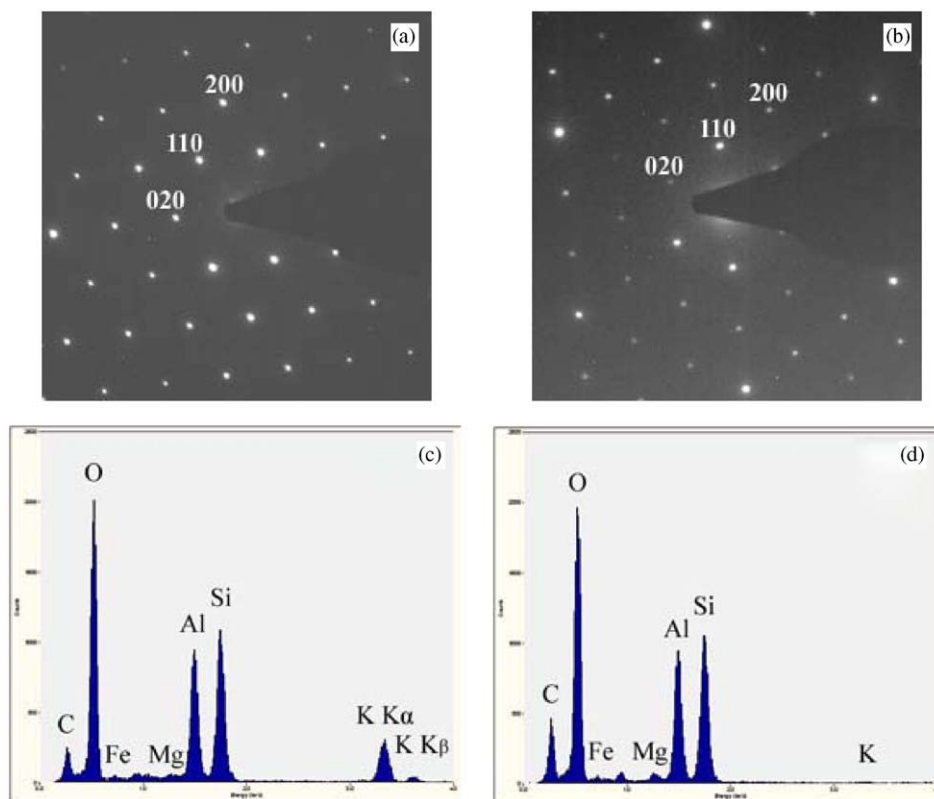


Fig. 3. The SAED of $(hk0)$ diffraction patterns and EDX spectra: (a) SAED of original muscovite, (b) SAED of muscovite after the seventh LiNO₃ treatment, (c) EDX of original muscovite, (d) EDX of muscovite after the seventh LiNO₃ treatment.

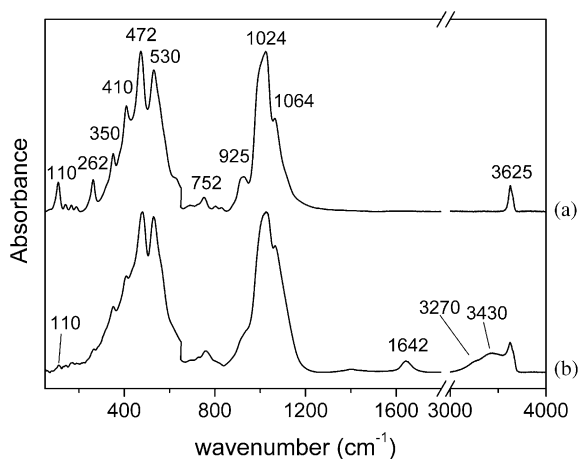


Fig. 4. The far-infrared and middle-infrared spectra of (a) original muscovite and (b) muscovite after the seventh LiNO₃ treatment.

Table 3
The assignment of infrared spectrum of original muscovite and muscovite after the seventh LiNO₃ treatment

Frequency (cm ⁻¹)	Assignment
1024	Si–O stretching vibration
1064	Shoulder of Si–O stretching vibration
752	Al–O–Si in-plane stretching vibration
472	Si–O bending vibration
530	Si–O bending vibration
110	K ⁺
3625	OH stretching vibration
3430	H ₂ O stretching vibration
1642	H ₂ O bending vibration
3270	Overtone of H ₂ O bending vibration
925	OH in-plane libration
410	OH out-of-plane libration
350	Mixture of libration and translatory vibration of OH
262	Coupling of Si–O bending vibration and OH translatory vibration

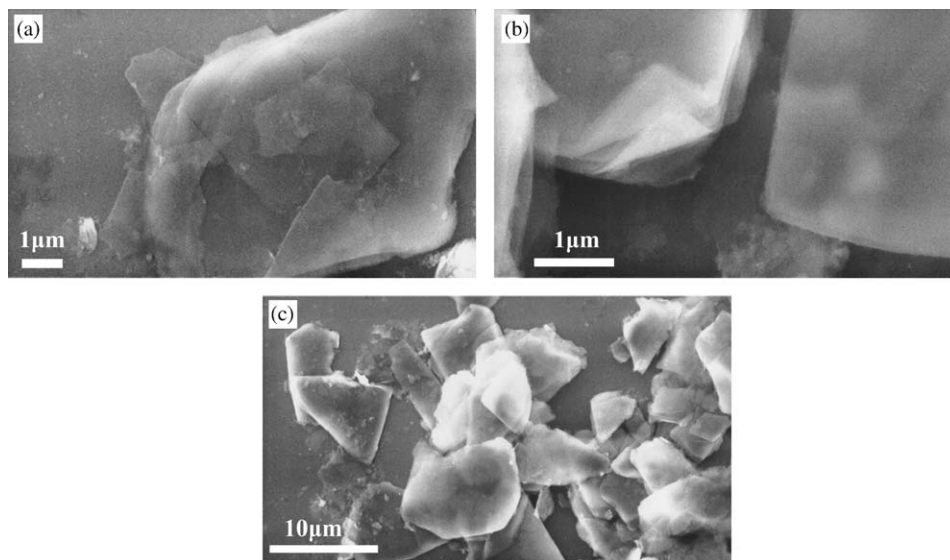


Fig. 5. The SEM images of (a) original muscovite, (b) muscovite after the second LiNO_3 treatment, and (c) muscovite after the seventh LiNO_3 treatment.

aluminosilicate skeleton has not been damaged and almost all the K^+ have been lost in the LiNO_3 treatments; furthermore, a large amount of water molecules have been adsorbed into the interlayer in the process.

To observe the morphology change of the product, scanning electron microscope images of original muscovite and Li-muscovite were obtained as shown in Fig. 5. We can see that the LiNO_3 treatments have little effect on the size of muscovite platelets. Furthermore, during the LiNO_3 treatment, it could be found that some of the muscovite particles were partially delaminated as shown in Fig. 5b. This phenomenon is consistent with the result that the specific surface area increased dramatically [18].

All the experiments mentioned above indicate that the LiNO_3 treatments did not affect the chemical composition and the structure of the aluminosilicate layer, and most of the K^+ in the interlayer were replaced by Li^+ ; in addition the interlayer spacing was expanded after the process. It seems that the increase of interlayer spacing is related to the exchange of K^+ by Li^+ in the interlayer. However, because the diameter of Li^+ is rather small compared with that of K^+ , it seems unreasonable that the increase of interlayer spacing results from the cation exchange. The infrared spectra (Fig. 4) show that a lot of water was adsorbed into the interlayer during the LiNO_3 treatments. Another dehydration experiment for the LiNO_3 -treated muscovite has been made as shown in Fig. 6. To remove the water, the LiNO_3 -treated muscovite was baked at 400°C for 6 h. After the dehydration treatment, the (00 l) diffraction peaks of the expanded interlayer spacing disappeared. Considering the infrared spectra and the strong hygroscopicity of Li^+ , it is very possible that after the exchange step of K^+ by Li^+ in the molten LiNO_3 treatment at 300°C , a lot of water entered the interlayer of muscovite in the next washing step and thus enlarged the interlayer spacing. Furthermore, we noticed that a weak

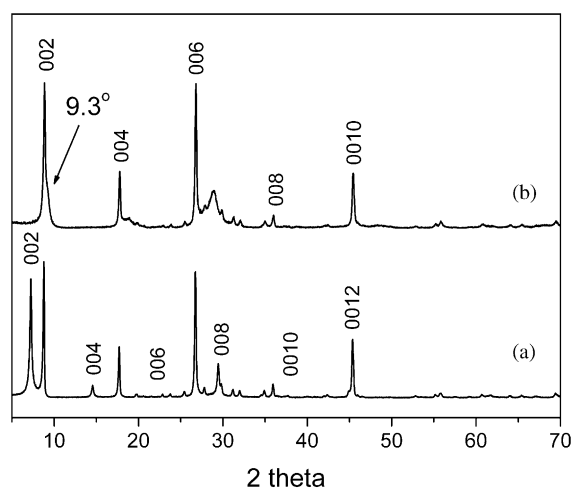


Fig. 6. The XRD diffraction patterns of (a) muscovite after the first LiNO_3 treatment and (b) sample a after dehydration treatment at 400°C for 6 h.

peak ($2\theta = 9.3^\circ$) appeared at the high angle region of (002) diffraction line in Fig. 6b. Its d value is about 9.51 \AA , which is smaller than the original muscovite (9.96 \AA). Because the diameter of Li^+ is smaller of K^+ , therefore a smaller interlayer spacing is expected after the dehydration. This phenomenon also happened in the synthetic mica. Keppler observed a similar interlayer distance expansion of synthetic Li dehydroxylated mica, which was exposed to humid air. It was found that the uptake of water was reversible at high temperature and loss of water results in a smaller interlayer distance [21]. Also we noticed that the relative intensities of (00 l) lines changed after dehydration. Compared with original muscovite, the cell parameter, the atom species, and the atom fractional coordinate, all changed. So the relative intensities of (00 l) diffraction lines are different from that of original muscovite. According

the loss amount in the calcination, the amount of water was calculated and shown in Table 2. There is about 1.32 water molecule in half unit cell in Li-muscovite.

4. Conclusion

After the LiNO₃ treatments, most of the K⁺ and Na⁺ in the interlayer space of muscovite were replaced by Li⁺. And because of the strong hygroscopicity of Li⁺, a large amount of water molecules entered the interlayer space. Therefore the spacing of (001) plane $d_{(001)}$ of muscovite was enlarged from 19.92 to 24.16 Å, which could allow for the intercalation of organic cations. Furthermore, during the preparation process, both the chemical composition and the structure of the aluminosilicate layer did not be affected.

Acknowledgment

This project was supported to National Natural Foundation of China (no. 29733080) and the Major State Basic Research Development Program (Grant no. G2000077503).

References

- [1] (a) T. Okada, T. Morita, M. Ogawa, *Appl. Clay Sci.* 29 (2005) 45–53;
(b) L.P. Meier, R. Nueesch, F.T. Madsen, *J. Colloid Interface Sci.* 238 (2001) 24–32;
(c) M.R. Stackmeyer, *Appl. Clay Sci.* 6 (1991) 39–57.
- [2] (a) T.J. Pinnavaia, *Science* 220 (1983) 365–371;
(b) J. Tudor, L. Willington, D. Ohare, B. Royan, *Chem. Comm.* 17 (1996) 2031–2032;
(c) T. Sivakumar, T. Krithiga, K. Shanthi, T. Mori, J. Kubo, Y. Morikawa, *J. Mol. Catal. A. Chem.* 223 (2004) 185–194.
- [3] E. Manias, G. Hadziioannou, G. Brinke, *Langmuir* 12 (1996) 4587–4593.
- [4] (a) Z. Wang, T.J. Pinnavaia, *Chem. Mater.* 10 (1998) 3769–3771;
(b) P.C. LeBaron, Z. Wang, T.J. Pinnavaia, *Appl. Clay Sci.* 15 (1999) 11–29.
- [5] (a) T. Tajima, N. Suzuki, Y. Watanabe, Y. Kanzaki, *Chem. Pham. Bull.* 53 (2005) 1396–1401;
(b) N. Suzuki, Y. Nakamura, Y. Watanabe, Y. Kanzaki, *Chem. Pham. Bull.* 49 (2001) 964–968;
(c) Y. Kanzaki, Y. Shimoyama, M. Tsukamoto, M. Okano, N. Suzuki, Y. Inoue, T. Tanaka, K. Koizumi, Y. Watanabe, *Chem. Pham. Bull.* 46 (1998) 1663–1666;
(d) C. Del Hoyo, V. Rives, M.A. Vicents, *Clays Clay Miner.* 44 (1996) 424–428.
- [6] (a) T. Seki, K. Ichimura, *Macromolecules* 23 (1990) 31–35;
(b) M. Ogawa, K. Kuroda, *Chem. Rev.* 95 (1995) 399–438.
- [7] (a) P. Capkova, H. Schenk, *J. Inclusion Phenom. Macrocyclic Chem.* 47 (2003) 1–10;
(b) G. Lagaly, A. Weiss, *Clays Clay Miner.* 20 (1972) 673;
(c) G. Lagaly, *Solid State Ionics* 22 (1986) 43;
(d) E. Hackett, E. Manias, E.P. Giannelis, *J. Chem. Phys.* 108 (1998) 7410–7415.
- [8] R.A. Vaia, R.K. Teukolsky, E.P. Giannelis, *Chem. Mater.* 6 (1994) 1017–1022.
- [9] M. Ogawa, K. Kuroda, *Bull. Chem. Soc. Jpn.* 70 (1997) 2593–2618.
- [10] (a) G.W. Brindly, G. Brown, *Crystal Structure of Clay Minerals and their X-ray Identification*; Mineralogical Society, Monograph no 5: London, 1980;
(b) A.C.D. Newman, *Chemistry of Clays and Clay Minerals*, Mineralogical Society, Monograph no 6: London, 1987.
- [11] J.J. Liang, F.C. Hawthorne, *Can. Miner.* 34 (1996) 115–122.
- [12] (a) M. Park, D.H. Lee, C.L. Choi, S.S. Kim, K.S. Kim, J. Choi, *Chem. Mater.* 14 (2002) 2582–2589;
(b) N. Suzuki, D. Yamamoto, N. Anaguchi, H. Tsuchiya, K. Aoki, Y. Kanzaki, *Bull. Chem. Soc. Jpn.* 73 (2000) 2599–2603;
(c) Y.S. Han, S.H. Choi, D.K. Kim, *J. Synchronr. Radiat.* 8 (2001) 731–733;
(d) E.R. Franklin, E. Lee, *J. Mater. Chem.* 6 (1996) 109–115.
- [13] (a) T. Kodama, M. Ueda, Y. Nakamuro, K. Shimizu, S. Komarneni, *Langmuir* 20 (2004) 4920–4925;
(b) K. Shimizu, K. Hasegawa, Y. Nakamuro, T. Kodama, S. Komarneni, *J. Mater. Chem.* 14 (2004) 1031–1035;
(c) T. Kodama, Y. Harada, M. Ueda, K. Shimizu, K. Shuto, S. Komarneni, *Langmuir* 17 (2001) 4881–4886;
(d) S.A. Stout, S. Komarneni, *J. Mater. Chem.* 13 (2003) 377–381;
(e) T. Kodama, K. Hasegawa, K. Shimizu, S. Komarneni, *Sep. Sci. Technol.* 38 (2003) 679–694;
(f) T. Kodama, S. Nagai, K. Hasegawa, K. Shimizu, S. Komarneni, *Sep. Sci. Technol.* 37 (2002) 1927–1942;
(g) T. Kodama, S. Komarneni, *Sep. Sci. Technol.* 35 (2000) 1133–1152.
- [14] (a) T. Kodama, S. Komarneni, *J. Mater. Chem.* 9 (1999) 533–539;
(b) T. Kodama, S. Komarneni, *Sep. Sci. Technol.* 34 (1999) 2275–2292.
- [15] G. Bracke, M. Satir, P. Kraub, *Clays Clay Miner.* 43 (1995) 732–737.
- [16] (a) W.R. Caseri, R.A. Shelden, U.W. Suter, *Colloid Polym. Sci.* 270 (1992) 392;
(b) L.P. Meier, R.A. Shelden, W.R. Caseri, U.W. Suter, *Macromolecules* 27 (1994) 1637–1642;
(c) M.A. Osman, C. Moor, W.R. Caseri, U.W. Suter, *J. Colloid Interface Sci.* 209 (1999) 232–239.
- [17] (a) M.A. Osman, G. Seyfang, U.W. Suter, *J. Phys. Chem. B* 104 (2000) 4433–4439;
(b) M.A. Osman, M. Ernst, B.H. Meier, U.W. Suter, *J. Phys. Chem. B* 106 (2002) 653–662;
(c) M.A. Osman, M. Ploetze, U.W. Suter, *J. Mater. Chem.* 13 (2003) 2359–2366;
(d) M.A. Osman, U.W. Suter, *J. Colloid Interface Sci.* 214 (1999) 400–406.
- [18] L. Zhao, X. Wang, N. Wu, Y. Xie, *Colloid Polym. Sci.* 283 (2005) 699–702.
- [19] V.C. Farmer, *The Layer Silicate in the Infrared Spectra of Minerals* Mineralogical Society, Mineralogical Society, London, 1974, pp. 331–363.
- [20] V. Laperche, R. Prost, *Clays Clay Miner.* 39 (1991) 281–289.
- [21] H. Keppler, *Am. Miner.* 75 (1990) 529–538.